

In situ measurements of erosion and redeposition during long duration discharges on TRIAM-1M

M. Sakamoto ^{a,*}, M. Ogawa ^b, H. Zushi ^a, A. Higashijima ^a, H. Nakashima ^a,
S. Kawasaki ^a, M. Hasegawa ^a, H. Idei ^a, K. Hanada ^a, K. Nakamura ^a,
K.N. Sato ^a, TRIAM Group

^a Advanced Fusion Research Center, Research Institute for Applied Mechanics, Kyushu University, Kasuga, Fukuoka 816-8580, Japan

^b Interdisciplinary Graduate School of Engineering Sciences, Kyushu University, Kasuga, Fukuoka 816-8580, Japan

Abstract

An in situ and real time measurement system of erosion and deposition has been developed, which is based on interference of light on a thin semi-transparent layer of redeposited material on substrate. It has been applied to long duration discharges in TRIAM-1M. The sapphire window is used as substrate. The deposition pattern on the window indicates up down and toroidal asymmetry. In the 5 h 16 min discharge, the thickness of the deposited layer increased monotonically with time and its deposition rate is $\sim 1.5 \times 10^{16}$ Mo m⁻² s⁻¹. In the low density and long duration discharge, the Mo deposition rate on the window depends on the ratio of Mo flux to hydrogen flux.

© 2007 Elsevier B.V. All rights reserved.

PACS: 52.40.Hf; 52.70.-m; 81.15.Cd

Keywords: Erosion/deposition; Redeposition; High-Z material; Sputtering; TRIAM-1M

1. Introduction

Understanding of the wall recycling is one of the most critical issues for achieving the steady state operation. Wall properties continue to change during a long duration discharge due to plasma–wall interactions such as erosion, redeposition and radiation damage. Codeposition of hydrogen with not only carbon atoms but also molybdenum atoms

eroded from the plasma facing components is recognized to play an important role in wall recycling [1–3].

The erosion and redeposition has been observed in many devices. Most of observations have been done in the post-mortem analysis. Also in TRIAM-1M ($R_0 \sim 0.84$ m, $a \sim 0.11$ m, stainless steel vacuum vessel, Mo poloidal limiters PLs and divertor plates DPs), Mo deposition was observed using a material probe in long duration discharges [3,4]. In order to understand deeper, in situ real time measurements of erosion and redeposition are highly desired. An in situ and real time measurement system based on

* Corresponding author. Fax: +81 92 573 6899.

E-mail address: sakamoto@triam.kyushu-u.ac.jp (M. Sakamoto).

interference of light on a thin semi-transparent layer of redeposited material has been developed, which was first developed in TEXTOR [5], and applied here to long duration discharges in TRIAM-1M.

2. Experimental set-up

Fig. 1 shows a schematic view of the erosion and deposition monitor (EDM) in TRIAM-1M. A sapphire window of 4 mm thickness is used as a substrate, which is also used for Thomson scattering measurement. It is located at about 75 mm away from the last closed flux surface of the plasma which lies at the center of PL. A fiber optic bundle which is composed of 450 optic fibers with the diameter of 100 μm is attached to the air side of the window. The optic fibers are mixed statistically. The fiber optic bundle is pushed on the window surface by spring action to avoid a gap between them due to vibration during the plasma production. Half of the optic fibers is used to illuminate the substrate with laser light (λ = 635 nm) and the other half guides the reflected light back to a photodiode. In order to avoid plasma light, an interference filter is mounted in front of the photodiode. The intensity

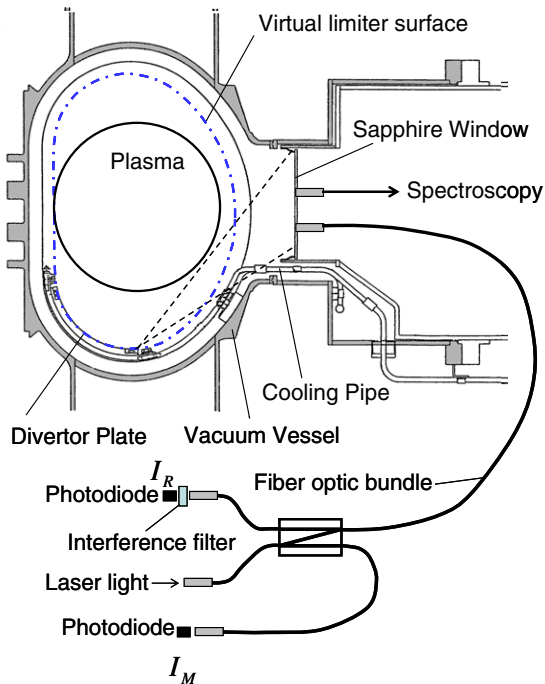


Fig. 1. A schematic diagram of the erosion and deposition monitor.

of the laser light is monitored by the other photodiode. The emission from the plasma is also measured at the same viewing port by a visible spectroscopy.

Part of the substrate is simply sketched in Fig. 2. Deposited layer is formed on the vacuum side of the substrate. Laser light of the intensity I_i penetrates the sapphire substrate (refractive index $n_0 = 1.77$) and is then partly reflected at the interface to the deposited layer (complex refractive index $n_1 + ik_1$) and at the interface of the deposited layer to vacuum ($n_2 = 1$). These two parts of the reflected light interfere. So the reflected intensity I_r depends on the thickness of the deposited layer d , the optical constants n_1, k_1 , the wavelength λ and the incident angle θ . In practice, multiple-beam interference occurs, and the reflectivity $R = I_r/I_i$ is written by the following equations:

$$R = |r|^2,$$

$$r = \frac{r_1 + r_2 \exp(-i\delta)}{1 + r_1 r_2 \exp(-i\delta)},$$

$$r_1 = \frac{n_0 - n_1}{n_0 + n_1}, \quad r_2 = \frac{n_1 - n_2}{n_1 + n_2},$$

$$\delta = \frac{4\pi}{\lambda} n_1 d \cos \theta.$$

In the case of TRIAM-1M, the deposited layer can be assumed to be Mo from the results of material probe experiments [6]. The value of $\cos \theta$ can be assumed to be unity, since the numerical aperture of the optic fiber is ~0.2, i.e. $\cos \theta \geq 0.98$. The reflectivity is shown in Fig. 3 as a function of thickness of Mo deposited layer. In the analysis of this paper,

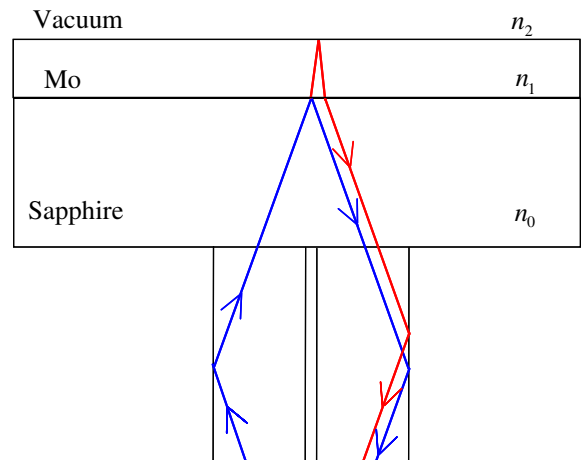


Fig. 2. A schematic diagram of basic idea of the measurement.

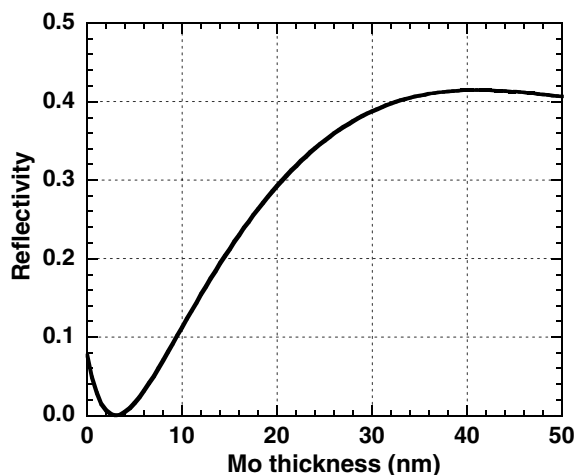


Fig. 3. Reflectivity as a function of Mo thickness on the sapphire window.

a complex refractive index of the Mo deposited layer is assumed to be that of bulk Mo, i.e. $n_1 = 3.68$ and $k_1 = 3.52$. If there was uncertainty of 10% in n_1 or k_1 , it gives error within about 10% to estimation of thickness of the deposited layer. Exact estimation of the complex refractive index of the deposited layer is in the future work.

3. Experimental results and discussions

Fig. 4 shows a deposition pattern on the sapphire window viewed from the air side after the experimental campaign with the period of 1.5-month in TRIAM-1M (the last campaign in 2005). The measurement position of EDM is indicated by the cross. It can be seen that the thickest part of the deposited layer (>20 nm) is located at the lower left and the deposition pattern is asymmetric relative to the mid-plane of the vacuum vessel. The source of Mo impurity is considered to be DP, since the observed MoI intensity shows up down asymmetry [7]. The observed ion temperature profile is also up down asymmetry due to downward $B \times \nabla B$ drift [8]. Charge exchange (CX) neutral hydrogen sputters Mo at DP and some of Mo atoms sputtered can reach the sapphire window, since the ionization mean free path of a Mo atom in SOL is simply calculated to be ~ 7 cm using typical SOL parameters of low density and long duration discharge. Because the Mo atom which reaches more upper of the window passes in higher density and higher temperature region and its pass length becomes longer, therefore

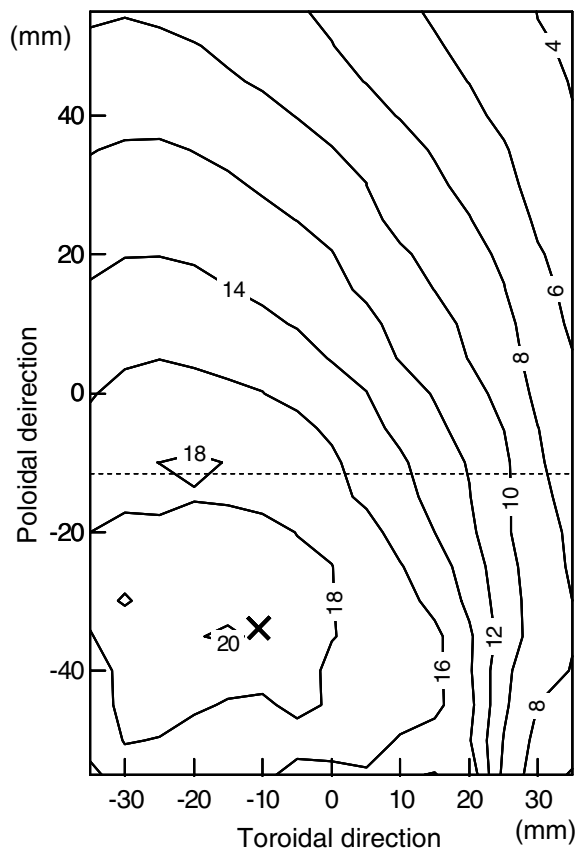


Fig. 4. Deposition pattern of Mo on the sapphire window. The dotted line indicates the mid-plane of the vacuum vessel. The number on the solid line indicates the thickness of the deposited layer.

the number of Mo atoms which can reach upper of the window is less than that of the lower. This is a possible candidate of reasons for up down asymmetry of the deposition pattern. As for the toroidal direction, the deposition pattern is weighted toward the ion drift side. This may suggest anisotropic sputtering in the toroidal direction.

Fig. 5 shows time evolution of thickness of the deposited layer on the sapphire window during six discharges including the interval time between discharges. The last discharge duration is 5 h 16 min. The growth of Mo deposit can successfully be measured using EDM. There is slow fluctuation within a few % in time evolution of thickness of the Mo deposit probably due to a very little fluctuation of wavelength of the laser. The thickness of the Mo deposit increases monotonically with time during the 5 h 16 min discharge and the averaged deposition rate is $\sim 1.5 \times 10^{16} \text{ Mo m}^{-2} \text{ s}^{-1}$. It is about much less than that of a material probe which is

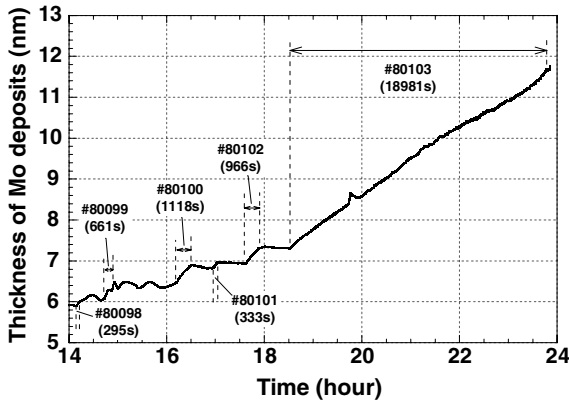


Fig. 5. Time evolution of the thickness of the deposited layer during 6-discharge operation including the interval time between discharges.

inserted ~ 5 mm away from the last closed flux surface of the plasma which lies at the center of PL [3]. In the 5 h 16 min discharge, the wall inventory obtained from particle balance analysis increased monotonically and the averaged wall pumping rate was $\sim 8.6 \times 10^{16} \text{ H m}^{-2} \text{ s}^{-1}$ [1]. Although the spatial deposition profile inside the vacuum vessel is necessary for quantitative analysis, monotonic increase of the deposited layer suggests that the continuous wall pumping is attributed to the codepositoin of hydrogen with eroded Mo.

In order to study parameter dependence of the deposition rate, a fueling rate was controlled to make the H_{α} intensity stepwise as shown in Fig. 6. Plasma with duration of 1200 s was sustained by 2.45 GHz lower hybrid current drive with the power of ~ 9.3 kW. The line averaged electron density is in the range of $(1.7\text{--}2.1) \times 10^{18} \text{ m}^{-3}$. The H_{α} intensity, MoI intensity and electron density seem to be correlated with each other. The OII intensity, however, continues to decrease with time although it changes according to the fueling rate. This decrease in the OII intensity has been studied in the reference [9]. As shown in Fig. 6(e), the thickness of the deposited layer increases with time and its increasing rate, i.e. deposition rate, seems to change relating to the H_{α} and MoI intensities. Fig. 7 shows a net deposition rate as a function of the ratio of Mo flux to hydrogen flux. It is found that the deposition rate increases with the ratio. The net deposition rate on the sapphire window is decided by both of flux of Mo atoms which are sputtered at DP and transport in SOL and erosion due to hydrogen CX neutrals. It should be noted that there exists no plasma

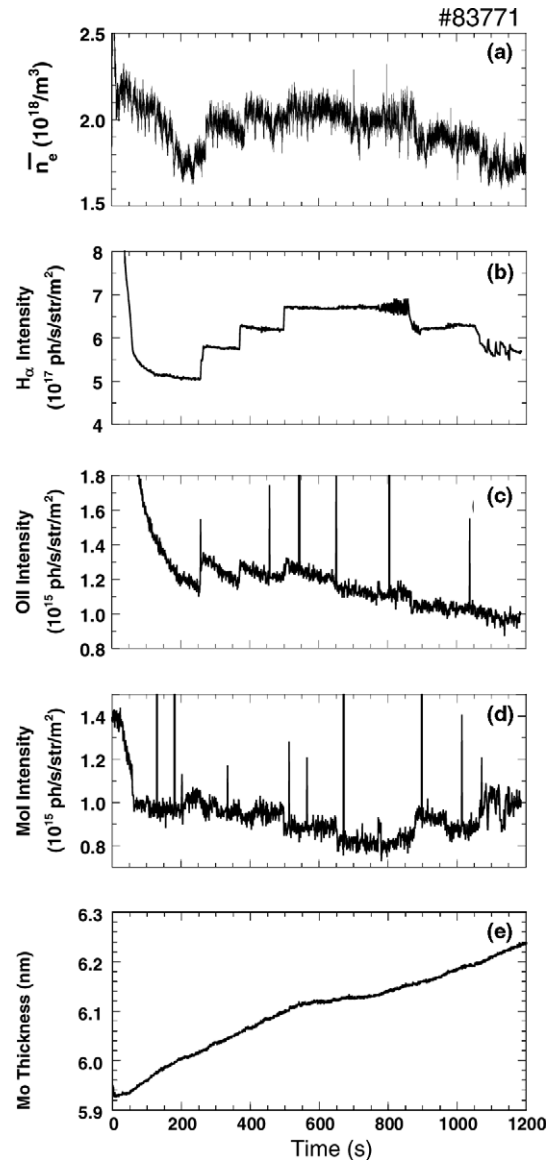


Fig. 6. Time evolution of (a) line averaged electron density, (b) H_{α} intensity, (c) OII intensity, (d) MoI intensity and (e) thickness of the deposited layer. The fueling rate is controlled to make the H_{α} intensity stepwise.

just in front of the sapphire window and no sputtering due to ions. The net deposition rate depends on plasma condition of core and SOL. We also observed the transition from net deposition to net erosion during a high density long duration discharge. The transition seems to relate to oxygen impurity flux. Although the quantitative analysis is future work, a useful tool to monitor erosion and deposition has been developed.

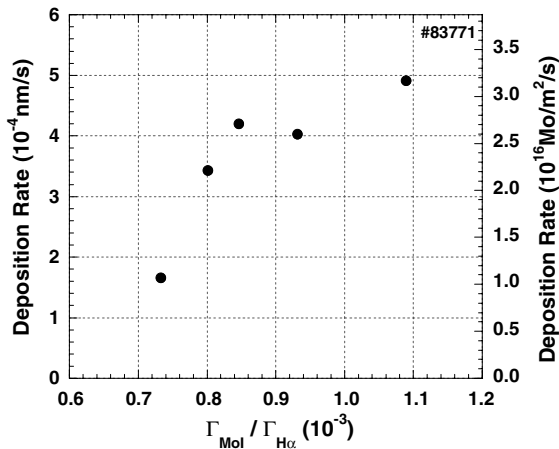


Fig. 7. Deposition rate as a function of the ratio of Mo flux to hydrogen flux to the plasma.

4. Summary

An in situ and real time measurement system of erosion and deposition has successfully been developed. It is based on interference of light on a thin semi-transparent layer of redeposited material on a substrate. It has been applied to long duration discharges in TRIAM-1M. A sapphire window for Thomson scattering measurement is used as the substrate. The deposition pattern on the sapphire window after the 1.5-month experimental campaign indicates up down and toroidal asymmetry. The divertor plate installed on the bottom of the vacuum vessel is responsible for the up down asymmetry. In an ultra-long duration discharge with duration of 5 h 16 min, the deposited layer grows monotonically

with time and the averaged deposition rate is $\sim 1.5 \times 10^{16}$ Mo m⁻² s⁻¹. It is the same trend as the increase in the wall inventory estimated from the particle balance analysis. In the low density and long duration discharge, the Mo deposition rate depends on the ratio of the Mo flux to the hydrogen flux.

Acknowledgements

The authors gratefully acknowledge helpful advices to develop the measurement system from Dr P. Wienhold. This work has been partially performed under the framework of joint-use research in RIAM Kyushu University and the bi-directional collaboration organized by NIFS. This work is partially supported by a Grant-in-Aid for Scientific Research from Ministry of Education, Science and Culture of Japan.

References

- [1] M. Sakamoto et al., in: Proceedings of the 32nd EPS Conference on Controlled Fusion and Plasma Physics, 2005, P5-005.
- [2] M. Sakamoto et al., Nucl. Fusion 44 (2004) 693.
- [3] M. Miyamoto et al., J. Nucl. Mater. 337–339 (2005) 436.
- [4] M. Tokitani et al., in: Proceedings of 12th ICFRM, Santa Barbara, 2005, 04–35.
- [5] F. Weschenfelder, P. Wienhold, J. Winter, J. Nucl. Mater. 196–198 (1992) 1101.
- [6] T. Hirai et al., J. Nucl. Mater. 283–287 (2000) 1177.
- [7] H. Zushi et al., Nucl. Fusion 45 (2005) S142.
- [8] H. Zushi et al., Nucl. Fusion 39 (1999) 1955.
- [9] M. Ogawa et al., J. Nucl. Mater., these Proceedings, doi:10.1016/j.jnucmat.2007.01.238.